JOURNAL
OF THE AMERICAN CHEMICAL SOCIETY
Registered in U.S. Patent Office. *© Copyright, 1975, by the American Chemical Society*

VOLUME 97, NUMBER 1 JANUARY 8, 1975

Constituent Analysis of the Potential Gradient Along a Reaction Coordinate. Method and an Application to CH_4 + T Reaction

Kenichi Fukui,* Shigeki Kato, and Hiroshi Fujimoto

Contribution from the Department of Hydrocarbon Chemistry, Kyoto University, Sakyo-ku, Kyoto, Japan. *Received June 18, 1974*

Abstract: On the basis of a formulation of the chemical reaction coordinate previously proposed the nuclear displacement on the reaction coordinate is discussed in terms of the potential energy gradient which is determined by the aid of the Hellmann–Feynman theorem from the electron density distribution and the nuclear arrangement of the total reacting system. The electron density is partitioned into several physically significant terms including exchange, delocalization, and polarization densities by the use of configuration interaction procedure, so that the potential gradient is also divided into the corresponding terms to discuss the origin of the favorableness or unfavorableness of a reaction path. An application is made to the methane–tritium reaction by the employment of an *ab initio* unrestricted Hartree–Fock molecular orbital method. Theoretical information is obtained with regard to submolecular mechanisms of the reaction.

The molecular orbital (MO) theory has been utilized in multifarious fashions to interpret the process of chemical reactions from an early stage of its development.[1] Various theories of orientation[2a] and stereoselection[2] have been proposed essentially in the frame of the activation energy criterion.[1,2] A progress has been made in that the partitioning of interaction energy,[3] for instance into Coulomb, exchange, delocalization, and polarization energies,[3b] assisted us in understanding the nature of phenomena occurring on the reaction path. An MO theoretical reasoning was given to the concept of a "favorable" path. The important role of the electron delocalization through the interaction of particular MO's (*i.e.*, the highest occupied (HO) MO, the lowest unoccupied (LU) MO, and the singly occupied (SO) MO) has been recognized.[3,4]

The description of the chemical process employed in these studies has mostly involved some assumptions concerning the reaction path, *i.e.*, the change in molecular geometry of each reactant along the reaction path. But this would be known by obtaining theoretically the complete surface for the potential energy of the reacting system. Such calculations were performed by the use of semiempirical and *ab initio* MO procedures.[5] These studies afforded useful information with respect to the reaction path, activation energy, or height of other barriers, geometry of the transition state, and so on. The only difficulty in this method lies in the drawing of a multidimensional potential energy surface for rather complicated systems.

In view of these circumstances it is desirable to obtain directly the information concerning the process along the reaction path. Bader[6a] gave the force acting along the reaction coordinate and discussed the change of electron density distribution and molecular geometry. Bader and Chandra,[6b] with the use of very accurate wave functions, calculated the interatomic binding force in the hydrogen formation reaction by means of the Hellmann–Feynman theorem.[7] This theorem was applied by Nakatsuji[8] to the discussion of molecular geometry and to the chemical interaction by the use of a chemically intuitive partitioning of forces into atomic dipole, exchange, and gross charge forces. Wang and Karplus[9a] obtained the trajectory of the path of methane formation from CH_2 and H_2 by calculating directly the forces, without the use of the Hellmann–Feynman force, given from the CNDO[10] potential surface. McIver and Komornicki[9b] presented a method to search for the transition state geometry by calculating the potential gradients.

The advantage of the physical simplicity and visuality in such force calculations will be multiplied by the combination with the theoretical formulation of reaction coordinate.[11,4c] An information on the reaction path would be obtained without resort to the potential-surface calculation.

The present paper treats the nuclear displacement along the reaction coordinate, analyzing constituents of the potential energy gradient in terms of various modes of configuration interaction between reactant molecules. This is for the purpose of elucidating what is the most important factor for determining the favorable reaction path. An application is made to a simple system; *i.e.*, the substitution of a hydrogen atom of methane by tritium.[12]

$$CH_4 + T \longrightarrow CH_3T + H$$

Description of Reaction Coordinate

In order to describe a reacting system, the nuclei are commonly treated as material particles which follow classical mechanics. The trajectory is given as a solution of a set of Lagrange's equations of motion

$$\frac{d}{dt}\frac{\partial L}{\partial \dot{\xi}_i} - \frac{\partial L}{\partial \xi_i} = 0 \qquad (i = 1, 2, \ldots, f) \qquad (1)$$

where L is the Lagrangian, ξ_i and $\dot{\xi}_i$ are generalized coordinate and velocity, respectively, and f is the number of internal degrees of freedom. The Lagrangian is given as

$$L = (1/2)\sum_{i,j}^{f} a_{ij}(\xi)\dot{\xi}_i\dot{\xi}_j - W(\xi) \qquad (2)$$

in which W is the potential energy function and ξ stands for the set of ξ_i's. The coefficients a_{ij} in the quadratic form are easily obtained from the corresponding formula expressed in the Cartesian coordinates by eliminating the translations and the rotations of the whole system.

To solve eq 1, one must determine the initial condition. But the initial condition is associated with the statistical distribution of molecular states, and the solutions obtained, *i.e.*, trajectories, depend on the choice of initial conditions.[9] If we permit an infinitely slow motion of nuclei, one can get a unique trajectory. This definition of trajectory corresponds to the reaction coordinate which is imagined in the discussion of chemical reactions based on the enthalpy criterion. This was defined and named as the "intrinsic" reaction coordinate by one of the present authors.[11]

Direction of Nuclear Displacement. Let us consider one nonequilibrium point on the reaction coordinate. By solving eq 1 under the condition mentioned above, one can get the infinitesimal displacements of coordinates as the solution of the following simultaneous equations[13]

$$\frac{\sum_{j=1}^{f} a_{ij}(\xi)\Delta\xi_j}{\partial W/\partial \xi_i} = \text{const} \qquad (i = 1, 2, \ldots, f) \qquad (3)$$

where $\Delta\xi_i$ is the value of displacement of coordinate ξ_i. Furthermore, if we write the matrix (a_{ij}) as **A** and put **B** = $\mathbf{A}^{-1}$, eq 3 is transformed to

$$\frac{\Delta\xi_i}{\sum_{j=1}^{f} b_{ij}(\xi)\frac{\partial W}{\partial \xi_j}} = \text{const} \quad (i = 1, 2, \ldots, f) \qquad (4)$$

where b_{ij} is the matrix element to **B**. Thus, when one $\Delta\xi_i$ is determined, all other $\Delta\xi_j$'s $(j = i)$ are determined by eq 4 to give the direction of nuclear displacement.

Next, at an equilibrium point which corresponds to the initial, final, transition, or an intermediate state, the energy gradients $\partial W/\partial\xi_i$ vanish, and we can obtain $\Delta\xi_i$'s by simply putting

$$\frac{\partial W}{\partial \xi_i} \sim \sum_{j=1}^{f} \frac{\partial^2 W}{\partial \xi_i \partial \xi_j}\Delta\xi_j \quad (i = 1, 2, \ldots, f) \qquad (5)$$

in eq 4. Thus, it is shown that the reaction coordinate starts from one of the normal coordinates at an equilibrium point, provided that they are nondegenerate.

Intermolecular Interaction Mode. In order to calculate the energy gradient, we use the Hellmann-Feynman theorem

$$\frac{\partial W}{\partial \xi_i} = \langle\Psi|\frac{\partial H}{\partial \xi_i}|\Psi\rangle = \int \rho(1)\frac{\partial V_{\text{ne}}{}^{(1)}}{\partial \xi_i}\,\mathrm{d}\mathbf{r}(1) + \frac{\partial V_{\text{nn}}}{\partial \xi_i} \qquad (6)$$

where Ψ is the electronic wave function, H is the Hamiltonian, V_{ne} and V_{nn} are the electron-nuclear and the nuclear-nuclear potentials in H, respectively, and r implies the space variables. The diagonal element of the first-order density matrix is given as

$$\rho(1) = n_{\text{e}}\int \Psi^*\Psi \mathrm{d}s_1 \mathrm{d}\tau_2 \ldots \mathrm{d}\tau_{\text{ne}} \qquad (7)$$

in which n_{e} is the number of electrons of the system, and s and τ are the spin and the spin-space variables. It is well known that the Hellmann-Feynman relation holds only for the exact wave function or "stable" wave function like the exact Hartree-Fock approximation.[14]

In the treatment of a mutually interacting system, the wave function is conveniently approximated by a combination of configuration functions, corresponding to charge-transferred, locally excited, and various other configurations, which are represented in terms of the MO's of each reactant molecule.[15,16] This configuration interaction (CI) representation gives a chemically graspable picture concerning the nature of the intermolecular interaction and chemical reactions. The perturbation method[15] can be used for the system of weaker interactions, but for stronger ones the configuration analysis,[16] that is, the method using the Hartree-Fock wave function expanded in terms of such configuration functions, gave a more reliable result.[17]

In these considerations, the configuration analysis technique is employed also in the present treatment. Since the details of configuration analysis have been described previously,[17a,b] we present here the outline pertinent to the purpose to treat the (CH_4 + T) system. To calculate the wave function of open-shell system, we employ the unrestricted Hartree-Fock (UHF) method.[18] Performing the configuration analysis, we can represent the wave function of the reacting system, Ψ, in the following CI form

$$\Psi = C_0\Psi_0 + \sum_{1_\alpha}^{\text{uno}} C_{i_\alpha \to 1_\alpha}\psi_{i_\alpha - l_\alpha} + \sum_{k_\beta}^{\text{occ}} C_{k_\beta \to i_\beta}\psi_{k_\beta \to i_\beta} +$$
$$\sum_{k_\alpha}^{\text{occ}}\sum_{l_\alpha}^{\text{uno}} C_{k_\alpha \to l_\alpha}\psi_{k_\alpha \to l_\alpha} + \sum_{k_\beta}^{\text{occ}}\sum_{l_\beta}^{\text{uno}} C_{k_\beta \to l_\beta}\psi_{k_\beta \to l_\beta} + \ldots \qquad (8)$$

where 0 indicates the zero configuration, that is the original one, i_α and i_β are the occupied and unoccupied orbitals of tritium, and $k_{\alpha,\beta}$ and $l_{\alpha,\beta}$ mean an occupied and an unoccupied MO of methane, respectively. The symbols Σ^{occ} and Σ^{uno} imply the summation over occupied and unoccupied MO's, respectively, and $i_\alpha \to l_\alpha$, for instance, stands for the one α-electron transfer from the ith MO to the lth MO. The coefficients of eq 8, C_0, $C_{i\alpha \to l_\alpha}$, etc., are given in the same manner as in our previous papers[17] with some modifications characteristic to the UHF case.

Partitioning of Density Matrix. Using the CI representation of the wave function of the reacting system, eq 8, we construct the first-order density matrix which is directly connected with the energy gradient through the Hellmann-Feynman theorem. The electron density of the reacting system, $\rho(CH_4 + T)$, is first divided into two parts

$$\rho(CH_4 + T) = \{\rho(CH_4) + \rho(T)\} + \Delta\rho^{I} \qquad (9)$$

where $\rho(CH_4)$ and $\rho(T)$ are the densities of CH_4 are T in their isolated states, respectively. The term $\Delta\rho^{I}$ is the difference density which is caused by the effect of interference between two interacting species and is termed the interference density.[19] Integration over all space provides

$$\int \rho(CH_4)\mathrm{d}r = 10, \ \int \rho(T)\mathrm{d}r = 1 \qquad (10)$$

$$\int \Delta\rho^{I}\mathrm{d}r = 0 \qquad (11)$$

The interference density is further decomposed into the exchange, delocalization, polarization density, and so on.

$$\Delta\rho^{\mathrm{I}} = \rho_{\mathrm{K}} + \rho(\mathrm{CH_4T}\,|\,\mathrm{CH_4{}^-T^+}) + \rho(\mathrm{CH_4{}^-T^+}\,|\,\mathrm{CH_4{}^-T^+}) + \rho(\mathrm{CH_4T}\,|\,\mathrm{CH_4{}^+T^-}) + \rho(\mathrm{CH_4{}^+T^-}\,|\,\mathrm{CH_4{}^+T^-}) + \rho(\mathrm{CH_4T}\,|\,\mathrm{CH_4{}^*T}) + \rho(\mathrm{CH_4{}^*T}\,|\,\mathrm{CH_4{}^*T}) + \ldots \quad (12)$$

where the notation $\mathrm{CH_4{}^-T^+}$ implies the state of one-electron transfer from T to $\mathrm{CH_4}$, and $\mathrm{CH_4{}^*}$ stands for the monoexcited states of $\mathrm{CH_4}$. The definitions of specialized interference densities are as follows

exchange density

$$\rho_{\mathrm{K}} = \rho_{00} - \{\rho(\mathrm{CH_4}) + \rho(\mathrm{T})\} \quad (13)$$

delocalization density

cross terms

$$\rho(\mathrm{CH_4T}\,|\,\mathrm{CH_4{}^-T^+}) = 2\sum_{l_\alpha}^{\mathrm{uno}} C_0 C_{i_\alpha \to l_\alpha}(\rho^{\alpha}{}_{0,i_\alpha \to l_\alpha} - S^{\alpha}{}_{0,i_\alpha \to l_\alpha}\rho^{\alpha}{}_{00})$$

$$\rho(\mathrm{CH_4T}\,|\,\mathrm{CH_4{}^+T^-}) = 2\sum_{k_\beta}^{\mathrm{occ}} C_0 C_{k_\beta \to i_\beta}(\rho^{\beta}{}_{0,k_\beta \to i_\beta} - S_{0,k_\beta \to i_\beta}\rho^{\beta}{}_{00}) \quad (14)$$

pure terms

$$\rho(\mathrm{CH_4{}^-T^+}\,|\,\mathrm{CH_4{}^-T^+}) = \sum_{l_\alpha}^{\mathrm{uno}}\sum_{l_\alpha'}^{\mathrm{uno}} C_{i_\alpha \to l_\alpha} C_{i_\alpha \to l_\alpha'}(\rho^{\alpha}{}_{i_\alpha \to l_\alpha, i_\alpha \to l_\alpha'} - S^{\alpha}{}_{i_\alpha \to l_\alpha, i_\alpha \to l_\alpha'}\rho_{00})$$

$$\rho(\mathrm{CH_4{}^+T^-}\,|\,\mathrm{CH_4{}^+T^-}) = \sum_{k_\beta}^{\mathrm{occ}}\sum_{k_\beta}^{\mathrm{occ}} C_{k_\beta \to i_\beta} C_{k_\beta' \to i_\beta}(\rho^{\beta}{}_{k_\beta \to i_\beta, k_\beta' \to i_\beta} - S^{\beta}{}_{k_\beta \to i_\beta, k_\beta' \to i_\beta}\rho_{00}) \quad (15)$$

polarization density

cross term

$$\rho(\mathrm{CH_4T}\,|\,\mathrm{CH_4{}^*T}) = 2\left\{\sum_{k_\alpha}^{\mathrm{occ}}\sum_{l_\alpha}^{\mathrm{uno}} C_0 C_{k_\alpha \to l_\alpha}(\rho^{\alpha}{}_{0,k_\alpha \to l_\alpha} - S_{0,k_\alpha \to l_\alpha}\rho^{\alpha}{}_{00} + \sum_{k_\beta}^{\mathrm{occ}}\sum_{l_\beta}^{\mathrm{uno}} C_0 C_{k_\beta \to l_\beta}(\rho^{\beta}{}_{0,k_\beta \to l_\beta} - S_{0,k_\beta \to l_\beta}\rho^{\beta}{}_{00})\right\} \quad (16)$$

pure term

$$\rho(\mathrm{CH_4{}^*T}\,|\,\mathrm{CH_4{}^*T}) = \sum_{k_\alpha, k_\alpha'}^{\mathrm{occ}}\sum_{l_\alpha, l_\alpha}^{\mathrm{uno}} C_{k_\alpha \to l_\alpha} C_{k_\alpha' \to l_\alpha'}(\rho^{\alpha}{}_{k_\alpha \to l_\alpha, k_\alpha' \to l_\alpha'} - S^{\alpha}{}_{k_\alpha \to l_\alpha, k_\alpha' \to l_\alpha'}\rho_{00}) + \sum_{k_\beta, k_\beta'}^{\mathrm{occ}}\sum_{l_\beta, l_\beta'}^{\mathrm{uno}} C_{k_\beta \to l_\beta} C_{k_\beta' \to l_\beta'} \times (\rho^{\beta}{}_{k_\beta \to l_\beta, k_\beta' \to l_\beta'} - S_{k_\beta \to l_\beta, k_\beta' \to l_\beta'}\rho^{\beta}{}_{00}) \quad (17)$$

where ρ^α and ρ^β are the α-spin and β-spin components of density, respectively. The other kinds of terms of smaller contributions are neglected since the terms taken above can always cover large fractions of the total density (see Table III).

In eq 13–17[20]

$$\rho^{\alpha}{}_{00} + \rho^{\beta}{}_{00} = n_{\mathrm{e}}\int \Psi_0{}^*\Psi_0 \mathrm{d}s_1 \mathrm{d}\tau_2 \ldots \mathrm{d}\tau_{n_{\mathrm{e}}} \quad (18)$$

$$\rho^{\alpha}{}_{0,i_\alpha \to l_\alpha} + \rho^{\beta}{}_{0,i_\alpha \to 1_\alpha} = n_{\mathrm{e}}\int \Psi_0{}^*\Psi_{i_\alpha \to l_\alpha} \mathrm{d}s_1 \mathrm{d}\tau_2 \ldots \mathrm{d}\tau_{n_{\mathrm{e}}} \quad (19)$$

$$\rho^{\alpha}{}_{i_\alpha \to l_\alpha, i_\alpha \to l_\alpha'} + \rho^{\beta}{}_{i_\alpha \to l_\alpha, i_\alpha \to l_\alpha'} = n_{\mathrm{e}}\int \Psi_{i_\alpha \to 1_\alpha}\Psi_{i_\alpha \to l_\alpha'} \mathrm{d}s_1 \mathrm{d}\tau_2 \ldots \mathrm{d}\tau_{n_{\mathrm{e}}} \quad (20)$$

and

$$S_{0,i_\alpha \to l_\alpha} = \int \Psi_0{}^*\Psi_{i_\alpha \to l_\alpha} \mathrm{d}\tau \quad (21)$$

The physical meaning of these interference densities is easily understood. Also each density vanishes upon integration over the whole space.

Using the Hellmann–Feynman theorem, we can divide the energy gradient in terms of the contribution of each electron configuration. The quasi-classical contribution, $\rho(\mathrm{CH_4}) + \rho(\mathrm{T})$, is partitioned into two parts: the intramolecular and the intermolecular Coulombic parts. The nuclear part of the Hellmann–Feynman force is also divided into the intramolecular and the intermolecular contributions. The interference density is decomposed into various contributions according to the density partitioning. The formulation of these partitioned energy gradients is made in a straightforward fashion and is not given.

Result of Calculation

Some MO calculations (CNDO and extended Hückel) have been carried out on the potential energy surface for the $\mathrm{CH_4}$ + H system and the results have been compared with respect to several different types of reaction, *i.e.*, abstraction, substitution, and so forth.[21] Recently *ab initio* calculations for this system were performed by Morokuma and Davis[22a] (RHF) and Ehrenson and Newton[22b] (UHF), and the potential energy surface was obtained to get reliable values of the transition state geometry and energy differences between these types of reactions. These studies suggest that the most favorable type of reaction is abstraction. Experimental results show that the normal reaction is abstraction and in high-energy conditions the substitution occurs additionally.

Notwithstanding these results, the present calculation is made with respect to substitution, since this is suitable for examining the utility of the method proposed. As the substitution, the inversion model is adopted here because the retention path requires much more energy than the former,[22a,b] although experimentally the occurrence of both inversion and retention is reported.[22c]

We first calculated the potential energy surface for this model by the UHF-MO method with the minimal basis set of Slater type orbitals (STO). The integrals are calculated by expanding STO's with three-term Gaussian functions (STO-3G).[23,24] The orbital exponents of STO's are 5.67 for C(1S), 1.72 for C(2S) and C(2P), and 1.18 for H(1S). The reacting system is assumed to maintain C_{3v} symmetry. Parameters used to describe the system are shown in Figure 1. The nonreactive C–H distances, $R_{\mathrm{CH_2}}$, $R_{\mathrm{CH_3}}$, and $R_{\mathrm{CH_4}}$, are fixed to be 1.097 Å throughout, which is the optimized value for the isolated methane molecule with the basis set used here. The two parameters, $\theta_{\mathrm{H_1CH_2}}$ and $R_{\mathrm{CH_1}}$, are optimized with respect to various C–T distances, $R_{\mathrm{C-T}}$. In Figure 2a, the minimum energy curve for R_{CT} is plotted. The calculated barrier height is 71.2 kcal/mol, which is comparable with the results of Morokuma and Davis.[22a,25] We show in Figure 2b the correlation of three parameters along the minimum energy reaction path. The geometry of the saddle point is calculated to be $R_{\mathrm{CT}} = R_{\mathrm{CH_1}} = 1.33$ Å, $\theta_{\mathrm{H_1CH_2}} = 90°$.

In order to calculate the direction of nuclear displacement, we must determine the internal coordinates. Although the number of internal degrees of freedom for the six-atomic system is 12 as indicated in Table I, we can reduce it to 4 (ξ_1, ξ_2, ξ_3, ξ_4) by the symmetry property of the reacting system. These four coordinates are not orthogonal to each other but are suitable for representing the nuclear rearrangements in this reaction model. If we assume that

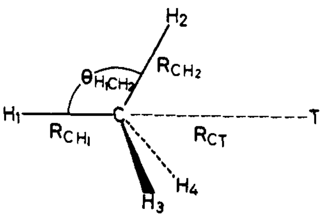

Figure 1. Model and parameters useα for the reacting system.

Table I. Twelve Internal Coordinates

$$\xi_1 = R_{\mathrm{CT}}$$

$$\xi_2 = \frac{1}{\sqrt{6}}(\theta_{\mathrm{H_1CH_2}} + \theta_{\mathrm{H_1CH_3}} + \theta_{\mathrm{H_1CH_4}} - \theta_{\mathrm{H_2CH_3}} - \theta_{\mathrm{H_3CH_4}} - \theta_{\mathrm{H_4CH_2}})$$

$$\xi_3 = R_{\mathrm{CH_1}}$$

$$\xi_4 = \frac{1}{\sqrt{3}}(R_{\mathrm{CH_2}} + R_{\mathrm{CH_3}} + R_{\mathrm{CH_4}})$$

$$\xi_5 = \frac{1}{\sqrt{6}}(2\theta_{\mathrm{TCH_2}} - \theta_{\mathrm{TCH_3}} - \theta_{\mathrm{TCH_4}})$$

$$\xi_6 = \frac{1}{\sqrt{2}}(\theta_{\mathrm{TCH_3}} - \theta_{\mathrm{TCH_4}})$$

$$\xi_7 = \frac{1}{\sqrt{6}}(2\theta_{\mathrm{H_1CH_2}} - \theta_{\mathrm{H_1CH_3}} - \theta_{\mathrm{H_1CH_4}})$$

$$\xi_8 = \frac{1}{\sqrt{6}}(2\theta_{\mathrm{H_2CH_3}} - \theta_{\mathrm{H_3CH_4}} - \theta_{\mathrm{H_4CH_2}})$$

$$\xi_9 = \frac{1}{\sqrt{2}}(\theta_{\mathrm{H_1CH_3}} - \theta_{\mathrm{H_1CH_4}})$$

$$\xi_{10} = \frac{1}{\sqrt{2}}(\theta_{\mathrm{H_3CH_4}} - \theta_{\mathrm{H_4CH_2}})$$

$$\xi_{11} = \frac{1}{\sqrt{6}}(2R_{\mathrm{CH_2}} - R_{\mathrm{CH_3}} - R_{\mathrm{CH_4}})$$

$$\xi_{12} = \frac{1}{\sqrt{2}}(R_{\mathrm{CH_3}} - R_{\mathrm{CH_4}})$$

tritium approaches the C atom by Δx, *i.e.*, $\Delta\xi_1 = \Delta x$ (<0), we can determine the displacements of the other three coordinates by eq 4. We calculated them at one point on the reaction coordinate where $\xi_1 = 1.6$ Å. The result is given in Table II. The relative nuclear displacements calculated from the potential energy relations of Figure 2 give results of $\Delta\xi_2/\Delta\xi_1 \sim 0.1$ and $\Delta\xi_3/\Delta\xi_1 \sim -0.3$ at $\xi_1 = 1.6$ Å, which are in good agreement with those values of Table II. This seems to imply that the Hellmann–Feynman theorem is sufficiently applicable to the present system which contains no lone-pair electrons and consists of several small atoms located around the central large atom. The direction of nuclear displacement climbing the potential barrier is opposite to that of the coupled force, $\Sigma_{j=1}^{12} b_{ij}(-\partial W/\partial\xi_j)$, and corresponds to the steepest ascending path on the potential energy surface. In general, the reacting system which involves an activation energy must ascend the potential energy barrier opposing the "forces." Actually, the energy which is needed to overcome the barrier is introduced from the kinetic energy of nuclei initially furnished.

Table II. Direction of Nuclear Displacement at $\xi_1 = 1.6$ Å[a]

	ξ_1	ξ_2	ξ_3	ξ_4
$\partial W/\Delta\xi_i$	0.04577	0.00597	−0.00788	0.00040
$\Sigma_{j=1}{}^{12} b_{ij}\frac{\partial W}{\partial\xi_j}$	0.05028	0.00479	−0.01240	0.00244
$\Delta\xi_i$	Δx	$0.0953\Delta x$	$-0.246\Delta x$	$0.0485\Delta x$

[a] The values in this table are given in atomic units.

It may be of interest to discuss the energy change caused by the infinitesimal nuclear displacement. On the reaction coordinate, S, both W and all ξ_1, ξ_2, ξ_3, and ξ_4 are functions of a single variable S; *i.e.*,

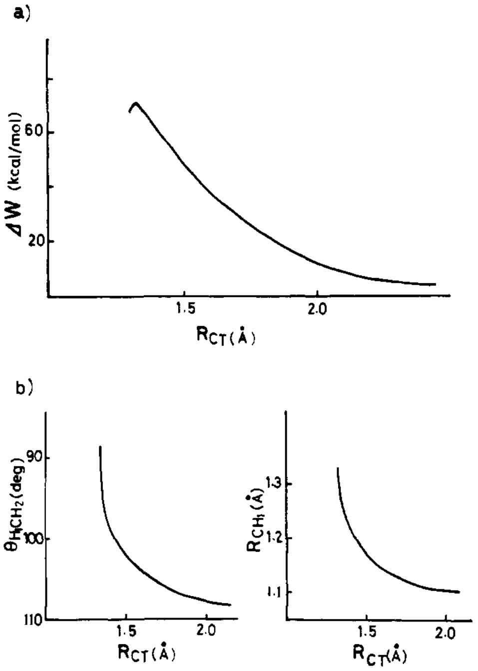

Figure 2. (a) Change of potential energy along the reaction path. (b) Correlations of three parameters.

$$W = W(S),\ \xi_1 = \xi_1(S),\ \xi_2 = \xi_2(S),\ \xi_3 = \xi_3(S),\ \xi_4 = \xi_4(S) \quad (22)$$

Hence, the small energy change on the reaction coordinate is written as

$$\Delta W = \frac{\mathrm{d}W}{\mathrm{d}S}\Delta S = \sum_{i=1}^{4}\frac{\partial W}{\partial\xi_i}\frac{\mathrm{d}\xi_i}{\mathrm{d}S}\Delta S = \sum_{i=1}^{4}\frac{\partial W}{\partial\xi_i}\Delta\xi_i \quad (23)$$

At the point $\xi_1 = 1.6$ Å, ΔW is calculated to be $0.0483\Delta x$ au ($30.3\Delta x$ kcal/mol) and its components are 28.7 Δx for ξ_4 in kcal/mol unit. The energy change associated with the tritium approach onto the carbon atom is largest at this point.

Origin of the Potential Energy Gradient

We have seen the acclivity of potential energy surface which the reacting system has to ascend to reach the transition state. We now analyze the slope of potential surface along the reaction coordinate in terms of the mode of intermolecular interaction and clarify the essential factors for raising and lowering the gradient.

Electronic Structure of the Reacting System. Before analyzing the potential energy gradient, we will give a brief discussion on the electronic structure of the reacting system. If we apply the configuration analysis, the CI representation of the wave function of the system contains all possible configurations in principle. Then we truncate the wave function to include the zero (original) and all one-electron transferred and all one-electron excited configurations. We collect contributions from the configuration functions of the same character in one term and express it in a more chemically graspable form. For example, the configuration wave function of one-electron transfer from tritium to methane is given as

$$\psi(\mathrm{CH_4{}^-T^+}) = \sum_{l_\alpha}^{\mathrm{uno}} C_{i_\alpha\to l_\alpha}\psi_{i_\alpha\to l_\alpha} \Big/ \left(\sum_{l_\alpha}^{\mathrm{uno}}\sum_{l_\alpha'}^{\mathrm{uno}} C_{i_\alpha\to l_\alpha}C_{i_\alpha\to l_\alpha'}S_{i_\alpha\to l_\alpha,\,i_\alpha\to l_\alpha'}\right) \quad (24)$$

Table III. Coefficients of Various Configuration Wave Functions

	2.0	1.8	1.6	1.4	1.35
$\psi(CH_4T)$	0.9855	0.9709	0.9376	0.8336	0.7028
$\psi(CH_4^-T^+)$	0.0316	0.0520	0.0892	0.1651	0.2153
$\psi(CH_4^+T^-)$	0.0569	0.0799	0.1132	0.1721	0.2222
$\psi(CH_4^*T)$	0.0141	0.0287	0.0612	0.1458	0.2341
Total wt	99.97	99.88	99.37	95.44	86.62

In Table III, the coefficients of various electronic configurations and the total weight of the limited number of CI wave functions taken there are shown for several values of ξ_1. These configurations cover the total weight of more than 99 except near the transition state. At an early stage of the reaction, the contributions from the transferred and the excited configurations are small (the former is the delocalization term and the latter is the polarization term). As the reaction proceeds, however, their contributions increase and the cross terms with the zero configuration become important. In particular the α-electron transfer from tritium to $4a_1$[26] unoccupied orbitals of the methane system and the β-electron transfer from $3a_1$ occupied orbital to tritium play dominant roles in the increase of the contribution of transferred configurations, which is shown in Figure 3. The MO's of deformed methane (C_{3v}) are also indicated in Figure 4. It is seen that the nodal property of unoccupied $4a_1$ orbital serves to weaken the C–H bond to be broken.

Energy Gradient. As shown in eq 23, the energy gradient along the reaction coordinate, S, can be divided into the terms which correspond to each internal coordinate. Therefore, we can examine them independently in relation to the electronic structure of the reacting system. In this system the sign of displacement is negative for $\Delta\xi_1$ and $\Delta\xi_2$ and positive for $\Delta\xi_3$, and hence the terms which contribute to making $(\partial W/\partial\xi_i)\Delta\xi_i$ negative are considered to lower the energy gradient and to make the reaction easier.

Table IV. Constituents of Energy Gradient with Respect to ξ_1

	1.8	1.6	1.4
Intramolecular	0.00047	0.00052	0.00060
Coulombic	0.00301	0.00556	0.00825
Exchange	0.02835	0.05616	0.09261
$(CH_4T\vert CH_4^-T^+)$	−0.00208	−0.00654	−0.01905
$(CH_4^-T^+\vert CH_4^-T^+)$	−0.00017	−0.00093	−0.00494
$(CH_4T\vert CH_4^+T^-)$	−0.00467	−0.00842	−0.01419
$(CH_4^+T^-\vert CH_4^+T^-)$	0.00023	0.00079	0.00275
$(CH_4T\vert CH_4^*T)$	0.00082	0.00342	0.01027
$(CH_4^*T\vert CH_4^*T)$	−0.00001	−0.00005	−0.00066

The first matter to be considered is the freedom of tritium approach to the carbon atom. We give the components of $-\partial W/\partial\xi_i$ at three points on the reaction coordinate, ξ_1 = 1.8, 1.6, and 1.4 Å in Table IV. It is shown in Table IV that the exchange term increases mainly the gradient, while the cross term of transferred configurations (of both directions of electron transfer) with the zero configuration contributes dominantly to lower it. In a neutral system such as CH_4 + T, as expected, the Coulombic interaction is not important. The cross term coming from excited configurations with the zero one acts as repulsive. The effects of the pure term of both the delocalized and the polarized structures are small in comparison with the cross terms. In order to clarify the different roles between the exchange term and the cross terms coming from the transferred and the zero configurations, the electron population of the reacting system may be partitioned according to the density partitioning mentioned above. The partitioned population at ξ_1 = 1.6 Å is shown in Table V. The exchange term yields a strong antibonding population in the carbon–tritium region, indicating the repulsion between the occupied orbitals. On the other hand, the cross terms create bonding components, which are mainly caused by the overlapping of the occupied orbitals of one subsystem with the unoccupied orbitals of the other. Consequently, the contribution of α-electron transfer is canceled by the exchange repulsion and the β-electron transfer plays a significant role for the new bond formation.[15c]

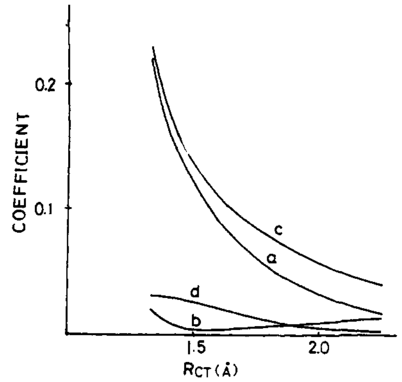

Figure 3. Change of coefficients of several transferred configurations along the reaction path: (a) from tritium 1s to $4a_1$ of C_{3v} methane; (b) from tritium 1s to $5a_1$ of C_{3v} methane; (c) from $3a_1$ of C_{3v} methane to tritium 1s; (d) from $2a_1$ of C_{3v} methane to tritium 1s.

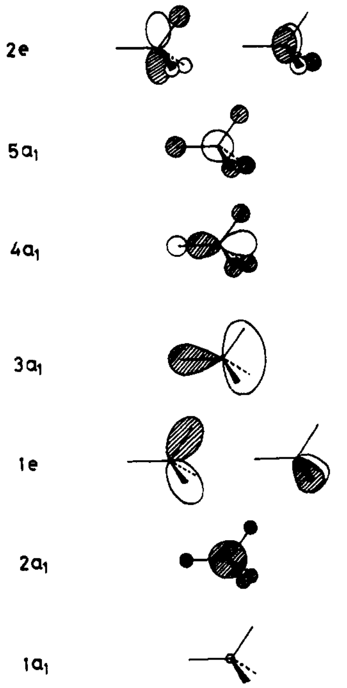

Figure 4. Schematic representation of MO's of C_{3v} methane.

Of interest next is the origin of Walden inversion. This is involved in the energy gradient with respect to ξ_2. The components of $-\partial W/\partial\xi_2$ are shown in Table VI. The exchange repulsion term extremely reduces the energy slope, which is caused by the strong antibonding densities between tritium and nonreactive hydrogen atoms. The contribution of the cross term of polarized configurations with the zero one causes the change of hybridization on the carbon atom and acts to promote the methyl inversion next to the exchange term. The exchange interaction is the intermolecular origin and the polarization is the intramolecular one for bringing about the Walden inversion. On the contrary, the deformed methane is forced to get loose to its equilibrium geometry. Hence the intramolecular contribution raises the energy gradient. The cross term coming from the configurations of electron-transfer from methane to tritium with the zero configuration creates the bonding components between tri-

Table V. Change of Electron Population due to the Interaction between CH_4 and T

	T	C	H_1	H_2
	(i) Atom Population			
$\rho(CH_4) + \rho(T)$	1.0	6.16273	0.97623	0.95368
ρ_K	0	−0.00800	+0.00685	+0.00038
$\rho(CH_4T\|CH_4^-T^+)$	−0.01120	−0.00094	+0.00819	+0.00132
$\rho(CH_4^-T^+\|CH_4^-T^+)$	−0.00796	+0.00501	+0.00256	+0.00013
$\rho(CH_4T\|CH_4^+T^-)$	+0.03241	−0.01319	−0.00994	−0.00309
$\rho(CH_4^+T^-\|CH_4^+T^-)$	+0.01282	−0.00646	−0.00401	−0.00078
$\rho(CH_4T\|CH_4^*T)$	0	−0.04349	+0.04255	+0.00031
$\rho(CH_4^*T\|CH_4^*T)$	0	−0.00008	+0.00007	+0.00001

	C–T	T–H_2
	(ii) Atom Bond Population Intermolecular	
$\rho(CH_4) + \rho(T)$	0	0
ρ_K	−0.20437	−0.04772
$\rho(CH_4T\|CH_4^-T^+)$	+0.06519	−0.01391
$\rho(CH_4^-T^+\|CH_4^-T^+)$	+0.00163	+0.00038
$\rho(CH_4T\|CH_4^+T^-)$	+0.04137	+0.00932
$\rho(CH_4^+T^-\|CH_4^+T^-)$	−0.00085	−0.00021
$\rho(CH_4T\|CH_4^*T)$	+0.00242	+0.00041
$\rho(CH_4^*T\|CH_4^*T)$	+0.00009	+0.00004

	C–H_1	C–H_2	H_1–H_2	H_2–H_3
	Intramolecular			
$\rho(CH_4) + \rho(T)$	0.72697	0.77348	−0.05624	−0.04036
ρ_K	−0.00467	0.02365	−0.00426	0.00378
$\rho(CH_4T\|CH_4^-T^+)$	0.00995	0.00339	−0.00447	0.00229
$\rho(CH_4^-T\|CH_4^-T^+)$	−0.00509	−0.00166	−0.00114	0.00010
$\rho(CH_4T\|CH_4^+T^-)$	−0.00174	−0.00715	0.00299	−0.00148
$\rho(CH_4^+T^-\|CH_4^+T^-)$	−0.00249	−0.00055	0.00054	−0.00017
$\rho(CH_4T\|CH_4^*T)$	−0.01738	0.00413	−0.00016	0.00014
$\rho(CH_4^*T\|CH_4^*T)$	−0.00518	−0.00063	−0.00011	−0.00008

Table VI. Constituents of Energy Gradient with Respect to ξ_2 (au)

	1.8	1.6	1.4
Intramolecular	0.01353	0.02540	0.04707
Coulombic	−0.00119	−0.00241	−0.00412
Exchange	−0.01448	−0.02027	−0.03101
$(CH_4T\|CH_4^-T^+)$	−0.00020	−0.00061	−0.00146
$(CH_4^-T^+\|CH_4^-T^+)$	−0.00027	−0.00094	−0.00313
$(CH_4T\|CH_4^+T^-)$	0.00271	0.00413	0.00438
$(CH_4^+T^-\|CH_4^+T^-)$	−0.00013	−0.00028	−0.00058
$(CH_4T\|CH_4^*T)$	−0.00365	−0.00651	−0.00865
$(CH_4^*T\|CH_4^*T)$	−0.00004	−0,00029	−0.00215

Table VII. Constituents of Energy Gradient with Respect to ξ_3 (au)

	1.8	1.6	1.4
Intramolecular	0.02717	0.04603	0.07275
Coulombic	0.00040	0.00056	0.00071
Exchange	0.00259	0.00419	0.00422
$(CH_4T\|CH_4^-T^+)$	−0.00073	−0.00114	−0.00148
$(CH_4^-T^+\|CH_4^-T^+)$	−0.00013	−0.00032	−0.00085
$(CH_4T\|CH_4^+T^-)$	−0.00203	−0.00354	−0.00588
$(CH_4^+T^-\|CH_4^+T^-)$	−0.00110	−0.00204	−0.00435
$(CH_4T\|CH_4^*T)$	−0.01583	−0.02838	−0.04976
$(CH_4^*T\|CH_4^*T)$	−0.00021	−0.00091	−0.00458

tium and nonreactive hydrogens, as shown in Table V, and is obstructive of the inversion.

Lastly, we examine the leaving of the hydrogen atom, H_1. The components of $\partial W/\partial \xi_3$ are shown in Table VII. The intramolecular charge distribution raises the gradient. The crossed product of the polarized configuration (the most contributing configuration is, of course, $3a_1 \rightarrow 4a_1$ (see Figure 4)) with the zero configuration plays the most important role to weaken the carbon-hydrogen bond. It is clear from Table V that this term decreases the carbon-hydrogen-1 overlap population most distinctly. The importance of the $3a_1 \rightarrow 4a_1$ excitation is easily seen from the characteristic feature of a radical reaction.

Notice should be taken here of the use of the Hellmann-Feynman theorem which yields a chemically graspable picture in the constituent analysis of energy gradient. As is well known, however, the condition to satisfy this theorem is very rigid. It is expected that any calculation with a limited basis set causes an appreciable error attributable to the nonsatisfaction of this condition. Nevertheless, we believe that the essential results obtained in the present paper will not be altered by the use of more rigorous calculations which are employable in principle with no difficulty except a larger consumption of computer time.

Acknowledgment. Authors express their appreciation to the Data Processing Center, Kyoto University, for generous permission to use the FACOM 230-75 computer.

References and Notes

(1) For instance, see A. Streitwieser, Jr., "Molecular Orbital Theory for Organic Chemists," Wiley, New York, N.Y., 1961.

(2) For instance, see (a) K. Fukui, "Theory of Orientation and Stereoselection," Springer-Verlag, Berlin, 1970; (b) R. B. Woodward and R. Hoffmann, "The Conservation of Orbital Symmetry," Academic Press, New York, N.Y., 1969, and the papers cited therein.

(3) (a) J. N. Murrell, M. Randic, and D. R. Williams, *Proc. Roy. Soc., Ser. A*, **284**, 566 (1965); (b) K. Fukui and H. Fujimoto, *Bull. Chem. Soc. Jap.*, **41**, 1989 (1968); (c) L. Salem, *J. Amer. Chem. Soc.*, **90**, 543, 553 (1968); A. Devaquet and L. Salem, *ibid.*, **91**, 3793 (1969); A. Devaquet, *Mol. Phys.*, **18**, 233 (1970); (d) G. Klopman, *J. Amer. Chem. Soc.*, **90**, 223 (1968); (e) R. Sustmann and G. Binsch, *Mol. Phys.*, **20**, 1, 9 (1971).

(4) (a) K. Fukui and H. Fujimoto, *Bull. Chem. Soc. Jap.*, **42**, 3399 (1969); (b) K. Fukui, "XXIII rd International Congress on Pure and Applied Chemistry," Vol. 1, Butterworth, London, 1971, p 65, and references cited therein; (c) K. Fukui, "Proceeding of the First International Conference on Quantum Chemistry," Reidel, 1974, p 113, and references cited therein.

(5) See, for instance (a) R. Hoffmann, R. Gleiter, and F. B. Mallory, *J. Amer. Chem. Soc.*, **92**, 1460 (1970); (b) K. Hsu, R. J. Buenker, and S. D. Peyerimhoff, *ibid.*, **94**, 5639 (1972); (c) J. A. Horsley, Y. Jean, L. Moser, L. Salem, R. M. Stevens, and J. S. Wright, *ibid.*, **94**, 279 (1972); (d) M. J. S. Dewar and M. C. Kohn, *ibid.*, **94**, 2704 (1972); (e) A. C. Trindle and D. D. Shillady, *ibid.*, **95**, 703 (1973); (f) P. Merlet, S. D. Peyerimhoff, R. J. Buenker, and S. Shih, *ibid.*, **96**, 959 (1974).

(6) (a) R. F. W. Bader, *Can. J. Chem.*, **40**, 1164 (1962); (b) R. F. W. Bader and A. K. Chandra, *ibid.*, **46**, 955 (1968).

(7) (a) H. Hellmann, "Einführung in die Quantenchemie," Deuticke, Leipzig, 1937; (b) R. P. Feynman, *Phys. Rev.*, **56**, 340 (1939); (c) for the applications and extensions of this theorem, see, *e.g.*, B. M. Deb, *Rev. Mod. Phys.*, **45**, 22 (1973).

(8) (a) H. Nakatsuji, *J. Amer. Chem. Soc.*, **95**, 345, 354, 2084 (1973); (b) H. Nakatsuji, *ibid.*, **96**, 24, 30 (1974).

(9) (a) I. S. Y. Wang and M. Karplus, *J. Amer. Chem. Soc.*, **95**, 8160 (1973); (b) J. W. McIver, Jr., and A. Komornicki, *ibid.*, **94**, 2625 (1972).

(10) J. A. Pople, D. P. Santry, and G. A. Segal, *J. Chem. Phys.*, **43**, S 129 (1965); J. A. Pople and G. A. Segal, *ibid.*, **43**, S 136 (1965).

(11) K. Fukui, *J. Phys. Chem.*, **74**, 4161 (1970).

(12) (a) R. Wolfgang, *Progr. React. Kinet.*, **3**, 97 (1965); R. Wolfgang, *Accounts Chem. Res.*, **2**, 248 (1969); **3**, 48 (1970); (b) R. W. Walker, *J. Chem. Soc. A*, 2391 (1968); (c) M. J. Kurylo and R. B. Timmons, *J. Chem. Phys.*, **50**, 5133 (1969); (d) C. C. Chou and F. S. Rowland, *ibid.*, **50**, 2763, 5133 (1969).

(13) This general eq 3 can be written[4c] in the form

$$\cdots = \frac{M_\alpha \Delta X_\alpha}{\partial W/\partial X_\alpha} = \frac{M_\alpha \Delta Y_\alpha}{\partial W/\partial Y_\alpha} = \frac{M_\alpha \Delta Z_\alpha}{\partial W/\partial Z_\alpha} = \cdots$$
$$(\alpha = 1, 2, \ldots)$$

by the use of usual three-dimensional Cartesian coordinates X_α, Y_α, and Z_α *for nucleus* α *of mass* M_α, in which the conditions of no translation nor rotation of the center of gravity

$$\sum_\alpha M_\alpha \Delta X_\alpha = \sum_\alpha M_\alpha \Delta Y_\alpha = \sum_\alpha M_\alpha \Delta Z_\alpha = 0$$

$$\sum_\alpha M_\alpha (Y_\alpha \Delta Z_\alpha - Z_\alpha \Delta Y_\alpha) = \sum_\alpha M_\alpha (Z_\alpha \Delta X_\alpha - X_\alpha \Delta Z_\alpha) = \sum_\alpha M_\alpha (X_\alpha \Delta Y_\alpha - Y_\alpha \Delta X_\alpha) = 0$$

are automatically satisfied since W is a function of internuclear distances only. The original equation given in ref 11 is obtained by the substitution

$$x_1 = M_1^{1/2}X_1,\ x_2 = M_1^{1/2}Y_1,\ x_3 = M_1^{1/2}Z_1,$$
$$x_4 = M_2^{1/2}X_2,\ x_5 = M_2^{1/2}Y_2,\ x_6 = M_2^{1/2}Z_3, \ldots$$

and this should have explicitly been specified there.

(14) (a) A. C. Hurley, "Molecular Orbitals in Chemistry, Physics, and Biology," P.-O. Löwdin and B. Pullman, Ed., Academic Press, New York, N.Y., 1964, p 161; (b) G. G. Hall, *Phil. Mag.*, **6**, 249 (1961).

(15) (a) H. Fujimoto, S. Yamabe, and K. Fukui, *Bull. Chem. Soc. Jap.*, **44**, 2936 (1971); **45**, 1566, 2424 (1972); (b) K. Fukui, H. Fujimoto, and S. Yamabe, *J. Phys. Chem.*, **76**, 232 (1972); (c) H. Fujimoto, S. Yamabe, T. Minato, and K. Fukui, *J. Amer. Chem. Soc.*, **94**, 9205 (1972).

(16) H. Baba, S. Suzuki, and T. Takemura, *J. Chem. Phys.*, **50**, 2078 (1969).

(17) (a) H. Fujimoto, S. Kato, S. Yamabe, and K. Fukui, *J. Chem. Phys.*, **60**, 572 (1974); (b) S. Kato, H. Fujimoto, S. Yamabe, and K. Fukui, *J. Amer. Chem. Soc.*, **96**, 2024 (1974); (c) S. Yamabe, S. Kato, H. Fujimoto, and K. Fukui, *Theor. Chim. Acta*, **30**, 327 (1973); (d) S. Yamabe, T. Minato, H. Fujimoto, and K. Fukui, *Theor. Chim. Acta*, **32**, 187 (1974).

(18) J. A. Pople and R. K. Nesbet, *J. Chem. Phys.*, **22**, 571 (1954).

(19) K. Ruedenberg, *Rev. Mod. Phys.*, **34**, 326 (1962).

(20) These hold the following relations in the UHF treatment:

$$\rho^{\beta}{}_{0,l_\alpha-l_\alpha} = S^{\alpha}{}_{0,l_\alpha-l_\alpha}\rho_{00},\ \rho^{\beta}{}_{l_\alpha-l_\alpha,l_\alpha'-l_\alpha'} = S_{l_\alpha-l_\alpha,l_\alpha'-l_\alpha'}\rho^{\beta}{}_{00},$$
$$\rho^{\alpha}{}_{0,l_\beta-l_\beta} = S^{\alpha}{}_{0,l_\beta-l_\beta}\rho_{00},$$

and

$$\rho^{\alpha}{}_{l_\beta-l_\beta,l_\beta'-l_\beta'} = S^{\alpha}{}_{l_\beta-l_\beta,l_\beta'-l_\beta'}\rho_{00}$$

(21) (a) J. J. Kaufmann, J. J. Harkins, and W. S. Koski, *Int. J. Quantum Chem., Symp.*, **1**, 261 (1967); (b) R. E. Qeston, Jr., and S. Ehrenson, *Chem. Phys. Lett.*, **9**, 351 (1971).

(22) (a) K. Morokuma and R. E. Davis, *J. Amer. Chem. Soc.*, **94**, 1060 (1972); (b) S. Ehrenson and M. D. Newton, *Chem. Phys. Lett.*, **13**, 24 (1972); (c) a referee kindly pointed out the experimental result of Professor Bunker.

(23) (a) K. O-ohata, H. Taketa, and S. Huzinaga, *J. Phys. Soc. Jap.*, **21**, 2306 (1966); H. Taketa, S. Huzinaga, and K. O-ohata, *ibid.*, **21**, 2313 (1966); (b) W. J. Hehre, R. F. Stewart, and J. A. Pople, *J. Chem. Phys.*, **51**, 2651 (1969).

(24) In the present calculation the expansion coefficients and the Gaussian orbital exponents are due to R. F. Stewart, *J. Chem. Phys.*, **52**, 431 (1970).

(25) For minimal basis set RHF-SCF calculation, 82.6 kcal/mol. For double ζ-SCF, 63.7 kcal/mol, and 41.7 kcal/mol for double ζ and CI calculation.

(26) The terminology of MO's of the methane part follows C_{3v} symmetry.

Geometries of Acetylene Ions[1]

San Yan Chu and Lionel Goodman*

Contribution from the Wright and Rieman Laboratories, School of Chemistry, Rutgers University, The State University of New Jersey, New Brunswick, New Jersey 08903.

Received May 31, 1974

Abstract: *Ab initio* SCF-MO calculations on the geometry of acetylene $^2\Pi_u$ cation, $^2\Pi_g$ anion, and $^1\Sigma_g$ neutral ground state using a double-ζ basis set are reported. The SCF calculation with double-ζ basis seems capable of reproducing accurately the ground state experimental geometry and reasonably the C–C and C–H stretching force constants. The anion is predicted to possess stable trans and cis isomers. From a Walsh type analysis the driving force for the bent geometry is found to be due to stabilization of the open shell π_g orbital through σ–π mixing. The $^2\Pi_u$ cation is predicted to be linear. The predicted equilibrium C–C bond lengthening is 0.05 Å for the cation and 0.08 Å for the anion relative to the ground state. The main reason for bond lengthening arises from removal of a bonding π_u electron on going to the cation and from addition of an antibonding π_g electron in the anion. The effects of electronic reorganization on the geometry are discussed. Principal results are that π_u is much more bonding in the cation than in the ground state, and wave functions which do not take into account electron recirculation predict the ionized state geometry poorly. The geometric rearrangement stabilization energy relative to vertical formation of the ions is -1.4 eV for the anion (leading to a predicted electron affinity of -1.3 eV) but only -0.12 eV for the cation. Thus Rydberg absorption spectra converging to the cation is predicted to have short vibrational progressions.

Recently we reported a near Hartree–Fock study of reorganization effects (orbital readjustment from the ground state) caused by π electron loss or capture in acetylene.[2] We discuss here the geometric rearrangements consequent to forming these ions. Because it is a simple polyatomic molecule containing π electrons with high symmetry, acetylene provides special interest in evolving and testing valence concepts. Indeed, a number of studies have been directed to that end.[3,4] A purpose of this study is to attempt to clarify the role that the effect of electronic reorganization from the ground state to the ionic states plays in geometric rearrangement. Additionally, reliable information concerning the equilibrium conformation for the cation will be useful in interpretation of Rydberg spectra, in the expectation that geometries of Rydberg states are mainly controlled by the valence electrons.

The three acetylene states studied are the $^1\Sigma_g$ ground state, the $^2\Pi_u$ cation $[(\sigma_{1g}{}^c)^2(\sigma_{1u}{}^c)^2(\sigma_{2g}{}^c)^2(\sigma_{2u}{}^c)^2(\sigma_{3g}{}^c)^2(\pi_u{}^c)^3]$, and the $^2\Pi_g$ anion $[(\sigma_{1g}{}^a)^2(\sigma_{1u}{}^a)^2(\sigma_{2g}{}^a)^2(\sigma_{2u}{}^a)^2(\sigma_{3g}{}^a)^2(\pi_u{}^a)^4(\pi_g{}^a)^1]$. The orbital forms at the minimal basis set level are discussed in ref 3d. We concluded in our reorganization studies that double-ζ level calculations can include most of the charge circulation effects accompanying ionization. Thus *ab initio* SCF calculations using MOLE programs[5a] were executed on IBM 360-67 and 91 systems with basis set D of ref 2. The calculations were carried out over a C–C and C–H bond distance mesh for a linear acetylene. The C–C–H angle was then allowed to vary using the optimized linear C–C and C–H bond distances. Besides geometry, the stretching force constants are also calculated.

In general, near Hartree–Fock wave functions predict molecular geometries closer to experimental values (within a few per cent) than they do vibrational frequencies (usually off by 20–30%);[5b] *i.e.*, Hartree–Fock wave functions are more capable of describing the position of a potential surface minimum than the shape in the vicinity of the minimum. We thus regard comparison of calculated and experimental ground state geometries as a test of the adequacy of the double-ζ basis set. Qualitative comparison of predicted force constants *vs.* the experimental values provides an additional test (see below).

$^1\Sigma_g$ Ground State

The predicted equilibrium C–C and C–H distances (Table I) for the ground state are 1.06 and 1.20 Å, respec-